Experimental Approach to Improve Canopy Area Estimation of Submerged Vegetation

Hyun Jung Cho[1], Duanjun Lu[2], James Kelley[1], and Lloyd McGregor[1]
[1]Department of Biology, Jackson State University, Jackson, MS 39217, USA
[2]Department of Physics, Atmospheric, Atmospheric Sciences, and Geoscience, Jackson State University, Jackson, MS 39217, USA

ABSTRACT

Remote detection of submerged plants is often limited due to the water absorption of Near Infrared (NIR) and the light scattering from suspended particles. Spectral variations along depth gradients were collected using a GER 1500 spectroradiometer over outdoor tanks that contain submerged plants. Field transect-surveys were also conducted in Grand Bay National Estuarine Research Reserve, Mississppi, to collect information on water depth and vegetation cover along depth gradients. The transect data were overlaid with airborne hyperspectral image in ArcGIS 9.2. Experimental study results indicated that the NIR region appears to have two peaks at approximately 710-720 nm and 810-820 nm in the submerged plants. Incorporation of these unique NIR reflectance peaks did not significantly improve detection of seagrass beds in turbid, high energy coastal waters, but, it appears to improve the use of hyperspectral aerial data in locating seagrass beds.

INTRODUCTION

Submerged aquatic vegetation (SAV) communities are an essential component in coastal and estuarine ecosystems. SAV beds play important role in reducing wave energy, enhancing sedimentation, stabilizing sediment, and supplying fisheries habitat, and serving as food sources for wildlife. Coastal SAV also improves water clarity by removing excessive nitrogen and phosphorus from water column and compete with algae. Therefore, studies of SAV distribution and abundance have become one of the interests of coastal scientists.

Remote sensing data have been used in studies of SAV and seagrasses distribution and abundance as s supplement or substitute of field surveys. Unlike remote sensing of terrestrial vegetation, the upwelling radiation from SAV has to cross the water column, which makes more complicated to process and interpret the data.

Chlorophyll *a* and *b* in green vegetation absorbs the most part of the energy in the visible wavelengths for photosynthesis; and healthy terrestrial vegetation is featured with a high reflectance in the near-infrared (NIR) region due to the spongy mesophyll structure. Spectral indices for vegetation, including Normalized Difference Vegetation Index (NDVI), have been created by utilizing these

characteristics of vegetation reflectance. However, the application of NDVI to SAV has been difficult due to the water absorption of NIR and reflection caused by varying water column constitutes. We used an experimental approach to understand the SAV's spectral reflectance pattern; compared them with field measured reflectance; identified the unique spectral regions for SAV that would improve detection and classification of seagrass beds using aerial hyperspectral data.

METHODS

Experimental setting

To obtain the spectral responses of SAV at varying water depths, a hand-held GER 1500 spectroratiomater was used to measure downwelling and upwelling energy from an outdoor tank that contain SAV (*Myriophlyllum aquaticum*) (Fig. 1). The experiments were conducted on clear days at near solar noon to minimize variability of solar elevation. The inside of the tank was lined with black plastic pond liners to minimize noise reflectance from the interior surface. The plants were planted at a density similar to the mean natural density during local growing season. The SAV tank was filled with clear water (local tap water) up to the depth of 50cm. The spectral measurements were made continuously as the tank water was siphoned out.

The spectral data were used for the computation of percent reflectance where Reflectance (%) = (Upwelling Radiance) / (Downwelling Irradiance) * 100 (Fig.2). Reflectance values were calculated only between 400-900 nm to eliminate low signal-to-noise data. Detailed characteristic reflectance curves for SAV at different water depths above the SAV canopy at different water turbidity of SAV were generated. The resulting data contained 315 bands within a range from 401 to 900 nm.

Figure 1. An experimental aquatic plant tank

Figure 2. Spectral reflectance patterns of the SAV planted bottom of the experimental tank

Field measurements of spectral data

Grand Bay National Estuarine Research Reserve (GBNERR) is located in southeast Mississippi (30.41° N; 88.53° W) (Fig.3). Spectral measurements were measured using the GER 1500 unit at 38 sites along four transects (Fig.4) that ran across Middle Bay in GBNERR on March 13th, 2007. At each site, water depth was measured using a wooden stick marked in one-foot increments; geographic coordinates were recorded using a GARMIN *etrex* handheld GPS; vegetation status including presence/absence and species was recorded; and upwelling energy was measured using a GER 1500 spectroradiometer. Sampling site number, latitude, longitude, turbidity value, water depth, vegetation species, and file number for spectral data were measured at each site; the data were saved in MS Excel (Fig.5) and added into ArcMap 9.2; and then point features were created from this file. The GER spectral reflectance data associated with the site numbers were saved in a separate file and imported into ArcMap (Fig. 6)

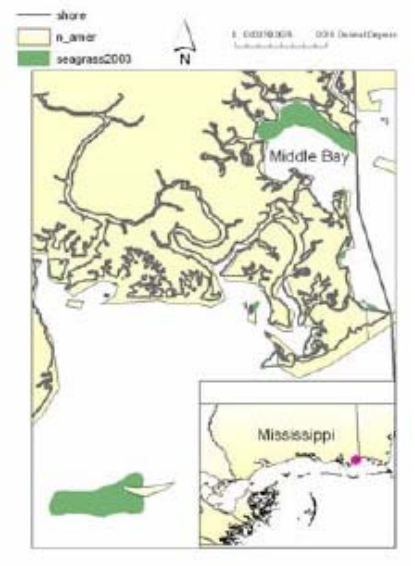

Figure 3. Map of Grand Bay National Estuarine Research Reserve, Mississippi, showing the locations of Middle Bay and seagrass beds.

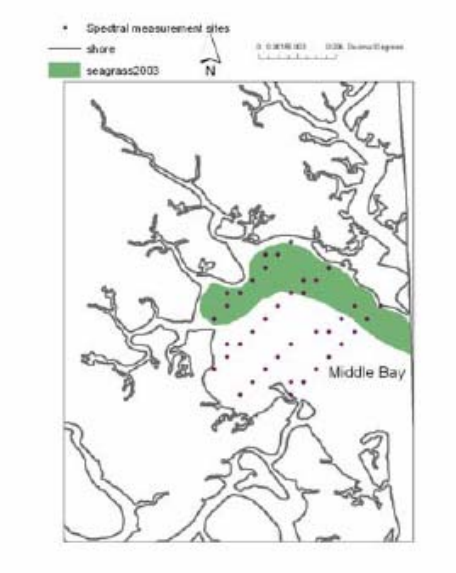

Figure 4. Spectral data sampling points in Middle Bay, Grand Bay NERR.

Site	Latitude	Longitude	Turbidity	Depth	Vegetation Type	GER file
1	30.38	-88.405	2.0	0.61	Algae	0.002
2	30.39	-88.406	12.0	0.08	Ruppia	0.011
3	30.39	-88.407	16.0	0.36	Ruppia	0.023
4	30.38	-88.407	10.0	0.46	Ruppia	0.031
5	30.39	-88.408	16.0	0.69	Halodule/Ruppia	0.038
6	30.39	-88.409	12.0	0.71	Ruppia/Algae	0.045
7	30.39	-88.410	12.0	0.76	Red/Brown Algae	0.052
8	30.39	-88.410	14.0	0.84	Algae	0.059
9	30.39	-88.411	16.0	1.09	Bottom Not Visible	0.066
10	30.39	-88.411	17.0	0.61	Algae	0.074
11	30.39	-88.410	22.0	0.76	No Vegetation	0.085
12	30.39	-88.410	27.0	0.84	No Vegetation	0.092
13	30.39	-88.409	16.0	0.69	Bottom Not Visible	0.099
14	30.39	-88.408	16.0	0.84	No Vegetation	0.106
15	30.39	-88.407	16.0	0.94	No Vegetation	0.113
16	30.39	-88.407	13.0	0.98	Algae/Hydroid	0.121
17	30.39	-88.406	16.0	0.61	Algae/Hydroid	0.135
18	30.39	-88.405	29.0	0.98	Ruppia/Algae	0.144

Figure 5. Data format of sampling site number, latitude, longitude, turbidity value, water depth, vegetation type, and file number for spectral data measured at each site

GER file	400.13	401.87	403.6	405.33	407.05	408.78	410.5	412.22
0.002	7.399654	7.376631	7.269366	7.501157	7.472445	7.550386	7.434925	7.403842
0.011	7.494538	7.483356	7.485011	7.679598	7.566851	7.603442	7.508694	7.523801
0.023	5.360624	5.472703	5.332913	5.382902	5.330344	5.462081	5.364106	5.273131
0.031	3.228671	3.242201	3.224524	3.222007	3.228123	3.252159	3.264717	3.229174
0.038	3.253464	3.165089	3.267606	3.242794	3.235949	3.28929	3.263041	3.265594
0.045	3.088877	3.130039	3.111848	3.076497	3.072187	3.137567	3.093795	3.088353
0.052	4.313256	4.32029	4.410273	4.476511	4.452109	4.356753	4.38031	4.457746
0.059	4.430341	4.410767	4.378237	4.493377	4.499867	4.501976	4.466859	4.46956
0.066	4.756917	4.902737	4.778685	4.946068	4.871319	4.847514	4.908141	4.847602
0.074	7.891644	7.802524	7.834719	7.858186	7.547719	7.535097	7.470247	7.514835
0.085	7.579546	7.626183	7.60507	7.809851	7.58949	7.419267	7.470247	7.514835
0.092	7.44158	7.476341	7.419761	7.493606	7.482401	7.337512	7.403113	7.482704
0.099	4.72387	4.832372	4.724378	4.758386	4.736167	4.782816	4.769567	4.76028
0.106	4.884631	4.704063	4.841883	4.76804	4.751131	4.87916	4.738423	4.736792
0.113	5.203166	5.223557	5.197763	5.228451	5.292154	5.21614	5.312821	5.255724
0.121	4.87817	4.822347	4.894776	4.746339	4.874925	4.875709	4.810582	4.837844
0.135	5.47025	5.525317	5.494677	5.610778	5.500689	5.545044	5.55493	5.559095
0.144	5.488244	5.492331	5.593352	5.594482	5.619018	5.536342	5.59401	5.622857
0.151	7.287668	7.36709	7.296806	7.294562	7.33251	7.330326	7.362749	7.379048

Figure 6. A sample of dataset of the spectral reflectance collected at the sampling sites in Middle Bay.

Airborne AISA hyperspectral acquisition

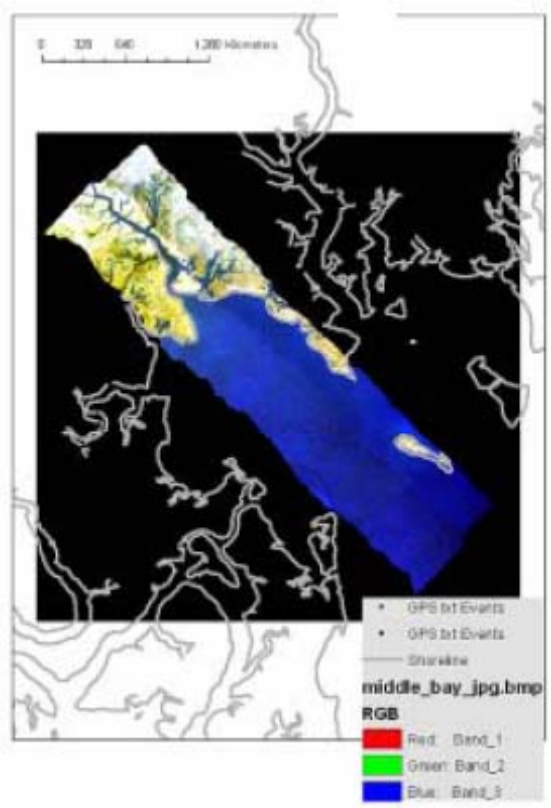

Aerial hyperspectral data were obtained in October 2003 over Grand Bay NERR (Fig.7). The data were obtained by AISA Eagle hyperspectral sensor by University of Nebraska at Lincoln's Center for Advanced Lane Management Information Technologies (CALMIT); and the data were available through CALMIT after pre-processed for atmospheric and geographic corrections. The Grand Bay NERR data had 20 hyperspectral bands within a range from 435 to 950 nm.

Figure 7. Flight lines of AISA Eagle hyperspectral data acquisition in October 2003 over Middle Bay, Grand Bay NERR.

Identification of critical wave bands

In order to reduce the redundancy and volume of the data, the following key spectral wavelengths (bands) were selected for SAV using experimental tank reflectance data (Table 1; Fig. 8).

Table 1. The key spectral wavelength ranges for unique SAV reflectance features.

GREEN	Green reflectance by plants	540 – 560 nm
RED	Red absorption regions by chlorophyll	670 – 690 nm
NIR1	The first peak in the near infrared	710 – 730 nm
NIR2	The dip in the Near Infrared	735 – 745 nm
NIR3	The second NIR peak	810 – 820 nm

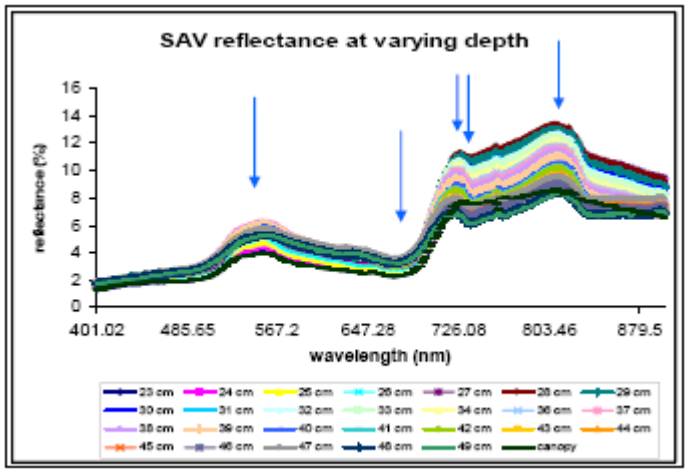

Figure 8. Spectral reflectance of SAV measured in the outdoor tank at varying depths. The selected wavelengths for SAV classification are indicated.

The field measured GER spectral reflectance (ground-truth data) and the AISA data at the selected wavelengths were extracted at the sampling sites (Fig. 4). Due to the time lag between the aerial data acquisition (October 2003) and the ground-truth measurements (March 2007) and the discrepancies in spectral resolutions between them, the direct comparison of spectral reflectance patterns did not provide meaningful results. Instead, the relationships among the key spectral wavelengths (Table 1) at varying depths were studied in order to find the AISA bands that can be used for SAV classification.

Supervised classification

Spectral Angle Mapping (SAM) was used to classify the AISA data. SAM is a classification technique based on the idea that observed reflectance spectrum can be considered as a vector in a multidimensional space where the number of dimensions equals the number of spectral bands (Lillesand, 2008). As described above, the experimental tank spectral data, field measured data, and AISA data were examined together by ratioing two pairs of the five key wavelengths (Table 1; Figure 8) to select three wavelength regions that appear to hold similar relationships among them. Only the three AISA bands whose centers are closest to the three wavelength regions (561nm, 710nm, and 819 nm) were used in SAM.

Bay-wide water depth data were downloaded from the National Geophysical Data Center website and converted to meters. Point features were created in ArcGIS using the data; and then interpolated using the Kriging method (the linear semivariogram model, using variable search radius) within the Spatial Analyst (Fig. 9). Along with the water depth data, previous surveyed seagrass transect data were used to select the ROI (endmembers) within the imagery.

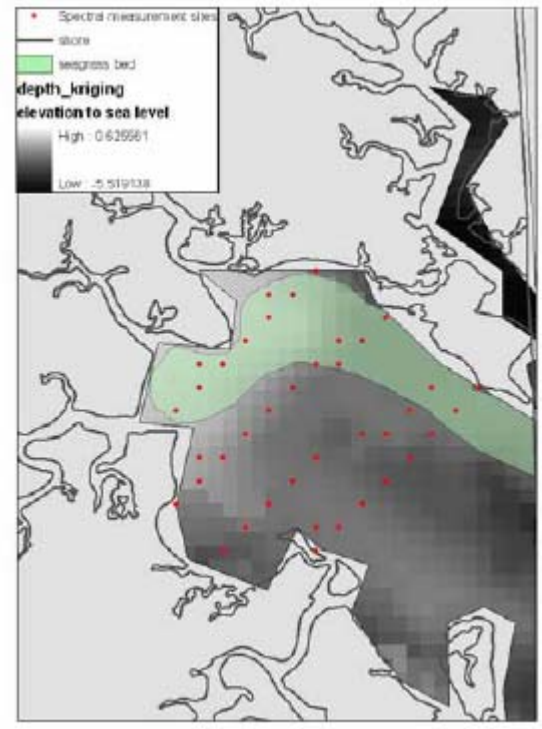

Fig. 9. Sampling sites for GER spectral data and seagrass bed location are overlaid with interpolated grid of water depth in Middle Bay.

Regions of Interests (ROIs) were selected as polygons to represent unvegetated deep water, shallow water SAV, marsh, and bare sand. The three AISA bands (561nm, 710nm, and 819 nm) were used to create an ENVI file in ENVI 4.1, then the three-band ENVI file was used for a supervised classification using SAM. The classified image was imported into ArcGIS and re-projected into UTM zone 16 (datum WGS 84) to be overlaid with spectral data and SAV survey data.

RESULTS and DISCUSSION

Selection of critical AISA bands for SAV detection

The direct comparison of experimental tank reflectance data, ground-truth field reflectance data, and air-borne AISA data were not possible, but all the datasets hold the truth that there are small peaks near 710-720 nm and 810-820nm and there is a reflectance dip in between those two wavelengths at around 740 nm (Fig 8 and Fig. 10).

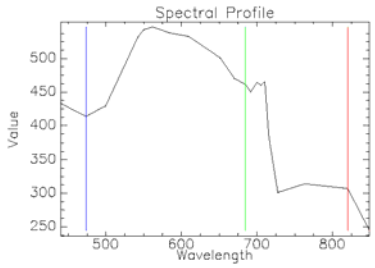

Figure 10. Spectral profile over an SAV bed captured by AISA imager.

Therefore, the NIR bands (centered at 710 nm and 819 nm) of AISA data were used to test if the visual distinction of vegetation signal from water would be improved (Fig. 11). Compared to the original image that contains all 20 bands (Fig.7), use of the NIR bands made the area that contain cholorophylls, both SAV (seagrass) beds and areas with high phytoplankton, more distinguishable (Fig. 11).

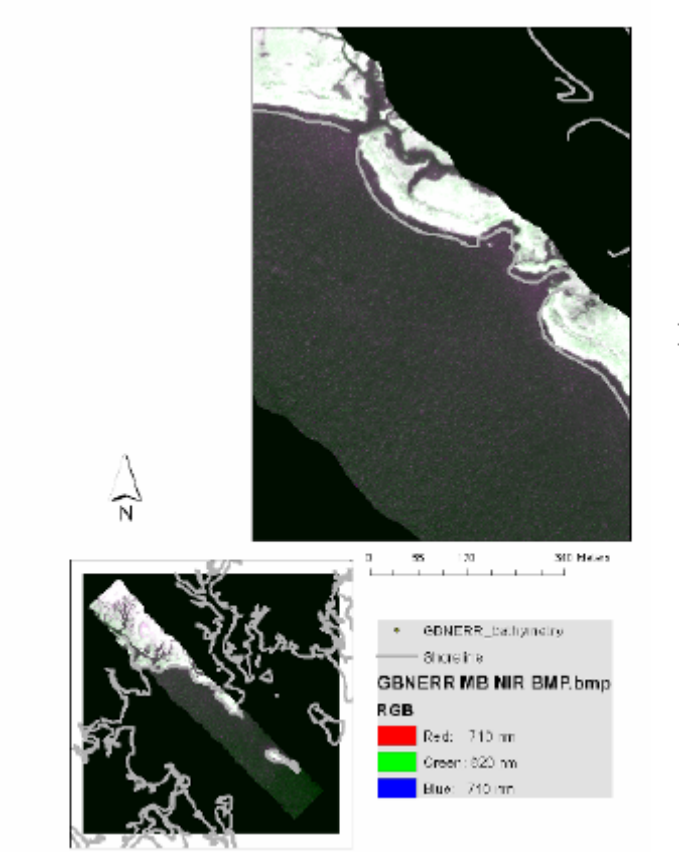

Figure 11. Shallow water SAV beds appear as purple.

SAM Classification

Fig. 12 shows the SAV classification of the AISA data. Although the shallow areas near the shore are correctly classified as SAV, the overall accuracy for class SAV was less than 20% when compared with our field transect SAV distribution data that we have been surveying every July and October since 2005. The transect SAV distribution and species composition can be found in Cho et al. (2007; http://gis.esri.com/library/userconf/proc07/papers/papers/pap_1043.pdf). The possible explanations for the low accuracy for SAV in Middle Bay are varying depth, high suspended particles that diminish signals from the substrates. The spectral signals from suspended phytoplankton that are similar to those of vascular plants probably introduced sources for the misclassifications.

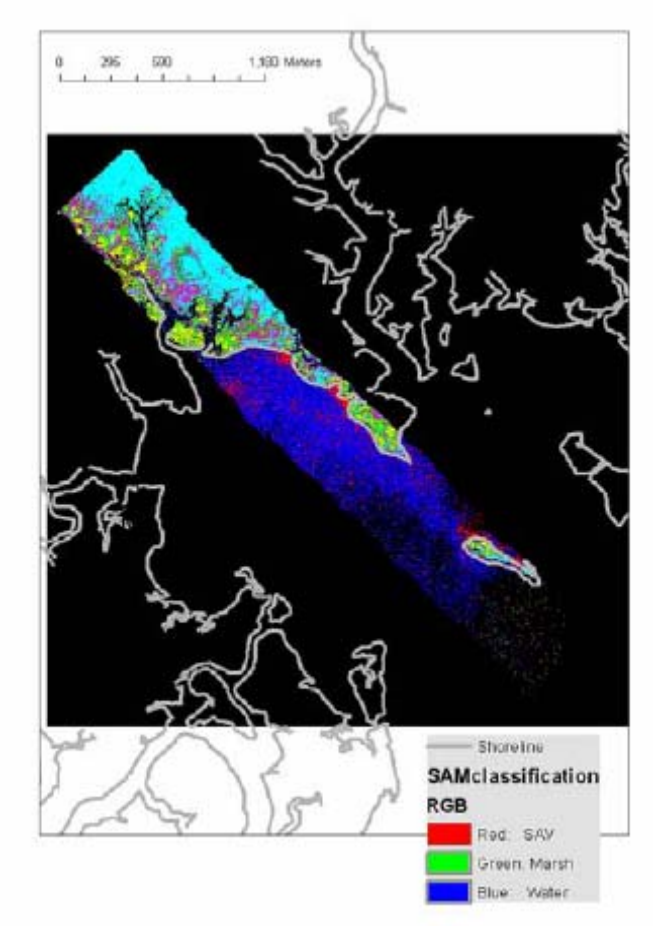

Figure 12. Result of SAM classification.

FURTHER STUDY

Aerial hyperspectral data were obtained in September 2006 over Apalachicola Bay. As opposed to the Grand Bay NERR data that had 20 hyperspectral bands, the Apalachicola data had 97 hyperspectral bands within a range from 435 to 950 nm. We used the same three AISA bands (561nm, 710nm, and 819 nm) to classify the data into 50 classes (Fig. 13). Although we have not done extensive GIS analyses on the preliminary data due to the lack of ground-truth data, the three band combination brought out even the deeper water vegetation in this relatively clear environment.

Therefore, we concluded that the incorporation of these unique SAV-NIR reflectance peaks did not significantly improve detection of seagrass beds in turbid, high energy coastal waters, but, it appears to improve the use of hyperspectral aerial data in locating seagrass beds.

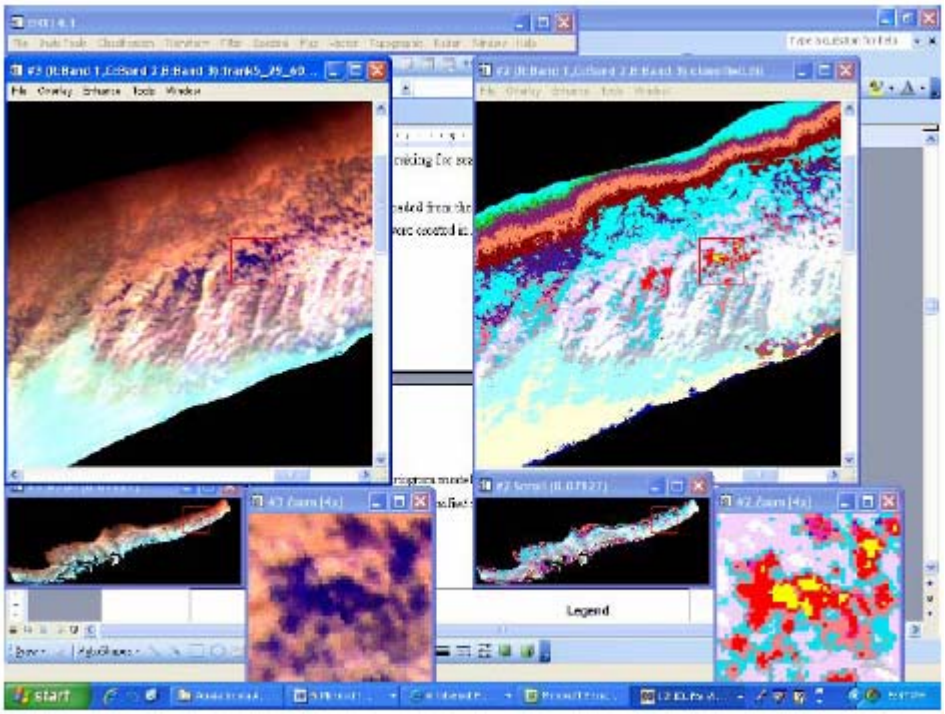

ACKNOWLEDGMENTS

This research is supported by grants from the National Geospatial-Intelligence Agency (NGA), NOAA-ECSC (Grant No.NA17AE1626, Subcontract # 27-0629-017 to Jackson State University), NSF-UBM, and NASA (Grant No. NNG05GJ72H/07-11-052, Agreement No. NNG05GJ72H). Authors appreciate Melissa Larmer, Jonathan Jones, and Fanen Kwembe who participated in experiments and field work and CALMIT, University of Nebraska, Lincoln. We thank to Chris May and Christina Watters for their significant involvement in and coordination of the field research at Grand Bay NERR.

LITERATURE CITED

- Cho, H.J., Melissa A. Larmer*, Jonathan R. Jones*, Christopher A. May, John Young. 2007. Use of GIS for Estuarine Seagrass Surveys and Restoration Planning. *Proceedings of International ESRI User Conference*. (http://gis.esri.com/library/userconf/proc07/papers/papers/pap_1043.pdf)
- Lillesand, T.M. and R.W. Kiefer, and J.W. Chipman. 2008. *Remote Sensing and Image Interpretation. 6th Edition*. Wiley. pp 768.

Corresponding Author:

Hyun J. Cho, Ph.D.
Assistant Professor
Department of Biology
Jackson State University
1400 Lynch St.
Jackson, MS 39217, USA
Tel: 601-979-3912
Fax: 601-979-5853
Email: hyun.j.cho@jsums.edu